Solution Photochemistry of Tetrakis(tetrabutylammonium) Decatungstate(VI) and Catalytic Hydrogen Evolution from Alcohols †

Toshihiro Yamase,* Naoki Takabayashi, and Masashi Kaji
Research Laboratory of Resources Utilization, Tokyo Institute of Technology, 4259 Nagatsuta, Midori-ku, Yokohama 227, Japan

Photoexcitation of the oxygen-to-metal charge-transfer band (323 nm, ε = 1.35 × 10^4 dm^3 mol^{-1} cm^{-1}) of $[NBu_4]_4[W_{10}O_{32}]$ in acetonitrile results in the reduction of W^{VI} to W^V [quantum yield, φ = (1—2) × 10^{-2}] with accompanying formation of 1-butene in less than stoicheiometric yield (70%). Prolonged irradiation leads to the accumulation of two-electron reduced species. The e.s.r. spectrum (g = 1.84, ΔH_{ms} = 20 G) of the photolyte is in good agreement with that of $[W_{10}O_{32}]^{5-}$. Flash photolysis experiments reveal that $[W_{10}O_{32}]^{5-}$ is produced by electron transfer from $[NBu_4]^+$ to $[W_{10}O_{32}]^{4-}$ within the lifetime of the photoflash ($t_{\frac{1}{2}}$ 50 μs) and that upon protonation $[W_{10}O_{32}]^{5-}$ undergoes disproportionation to yield the two-electron reduced and diprotonated species $[H_2W_{10}O_{32}]^{4-}$. The addition of water to the solvent results in a decrease in the rate of disproportionation of $[HW_{10}O_{32}]^{4-}$, a shift in the reduction potential of $[W_{10}O_{32}]^{4-}$ to more positive values, and the formation of butyraldehyde as an additional photoproduct. The significance of the highly negative oxidation potential for the photoreduced decatungstates $[W_{10}O_{32}]^{5-}$ and $[H_2W_{10}O_{32}]^{4-}$ is considered in connection with the photocatalytic evolution of H_2 from alcohols and their net oxidation to the corresponding aldehydes. U.v. irradiation of $[W_{10}O_{32}]^{4-}$ in the presence of heterogeneous catalysts such as RuO_2, IrO_2, and Pt leads to the evolution of H_2 from butanol (φ = 0.03) with a turnover of more than 100 at room temperature.

This study is a continuation of our investigation of the photochemistry of polyoxomolybdate with the goal of establishing the patterns of polyoxometalate photochemistry.[1-6] It has been reported that the photoirradiation of aqueous solutions containing alkylammonium polytungstate(VI) leads to H_2 evolution from water in a homogeneous system and the reaction mechanism has been discussed on the basis of the photochemistry of alkylammonium polymolybdate(VI).[1,2] Using isopropylammonium, $[NH_3Pr^i]^+$, as cation, photoexcitation of the oxygen-to-tungsten ligand-to-metal charge-transfer (l.m.c.t.) band allows the transfer of a hydrogen-bonded proton from $[NH_3Pr^i]^+$ to a bridging oxygen atom at an octahedral site of the polyoxo-anion and the subsequent redox reaction between polytungstate(VI) and water to yield W^V and $OH^{\cdot}$. In this case, $[NH_3Pr^i]^+$ is considered to serve mainly as an electron relay for the photoredox reaction, although it is oxidized to a small extent. Such photoreduced polytungstates exhibit oxidation potentials more negative than the reduction potential of water and lead to hydrogen generation as a result of the reduction of water coupled with the oxidation to W^{VI}.[5]

Polyoxotungstate(VI) is particularly interesting because of its possible use as a replacement for both the photosensitizer and methyl viologen (1,1′-dimethyl-4,4′-bipyridinium dichloride) in many model systems for the reduction of water.[7-10] Recently, photocatalytic redox reactions of alcohols in the presence of heteropolyoxotungstates such as $[SiW_{12}O_{40}]^{4-}$, $[PW_{12}O_{40}]^{3-}$, and $[P_2W_{18}O_{62}]^{6-}$ have been reported in the context of chemical conversion of solar energy.[11-14] We now report a quantitative photochemical study of tetrakis(tetrabutylammonium) decatungstate $[NBu_4]_4[W_{10}O_{32}]$ in CH_3CN and the usefulness of $[W_{10}O_{32}]^{4-}$ as a photocatalyst for H_2 production from water and alcohols. Since $[NBu_4]^+$ possesses no proton for hydrogen bonding with the polyoxo-anion, it is also interesting to know the effect of $[NBu_4]^+$ on the photoreactivity of $[W_{10}O_{32}]^{4-}$. It is well known that $[W_{10}O_{32}]^{4-}$ is identical with ' polytungstate-Y ' in acidic aqueous solutions and is reversibly electrochemically reduced to blue species in two successive steps in non-hydrolytic solvents.[15,16]

Experimental

Tetrakis(tetrabutylammonium) decatungstate was prepared according to Klemperer's method [17] and recrystallized from acetone–water (1 : 1 v/v) (Found: C, 22.85; H, 4.55; N, 1.70; W, 55.15. Calc. for $[NBu_4]_4[W_{10}O_{32}]$: C, 23.15; H, 4.35; N, 1.70; W, 55.4%). The salt was identified by its characteristic absorption maximum at 323 nm in CH_3CN (ε = 1.35 × 10^4 dm^3 mol^{-1} cm^{-1}), which corresponds to the oxygen-to-tungsten charge-transfer band. Tetrabutylammonium perchlorate as a supporting electrolyte for the electrochemical study was recrystallized twice from ethanol. All other reagents were at least analytical grade and were used as supplied. Removal of water from CH_3CN was carried out by stirring it on 5A molecular sieves and then filtering. The CH_3CN was then distilled from calcium hydride before use. All glassware was baked at around 150 °C prior to use.

A 500-W super-high-pressure mercury lamp in conjunction with filters was used as the light source. Light intensities at 365 nm were measured using potassium ferrioxalate actinometry.[18] Sample solutions (10 cm^3) in Pyrex tubes were deaerated with solvent-saturated nitrogen for the long-term photolyses. The solution containing the required amount of heterogeneous catalyst powder was continuously stirred during the photoirradiation.

Analysis of W^V in the photolyte was carried out at room temperature by titration of $KMnO_4$ under an atmosphere of nitrogen, which resulted in the disappearance of the blue colour due to W^V. Gas chromatography (Hitachi 164 instrument) and mass spectrometry (Hitachi M80 GC/MS spectrometer) were employed for analyses of 1-butene, butyraldehyde, tributylamine, and hydrogen; 1-butene and hydrogen were analyzed on Porapak N and Carbosieve S columns, respectively. The concentration of 1-butene in solutions was estimated to be about 3.7% of that in the gas phase. Butyraldehyde was determined by distilling the photolyte under reduced pressure at 50 °C and chromatographing on a Flusin T column. The residue was extracted with chloroform, and tributylamine and succinonitrile were detected by chromatography on a PEG 20M column. The formation of butyraldehyde was also confirmed by calorimetric quantitative analysis (at 600 nm).[19] Formaldehyde in photolytes was determined by means of

---

† *Non-S.I. units employed*: Torr = (101 325/760) Pa; G = 10^{-4} T.

Table 1. Quantum yields of photoproducts * for deaerated solutions containing 3 mmol dm^{-3} $[NBu_4]_4[W_{10}O_{32}]$ at room temperature

Solvent composition acetonitrile–water (v/v)	Irradiation time (h)	$10^3\,\varphi_{W^V}$	$10^3\,\varphi_{1\text{-butene}}$	$10^4\,\varphi_{CHO}$	$10^5\,\varphi_{amine}$
10 : 0	1	16	12		
	3	13	9.5	0	
	6	7.1	4.9	0	21
9 : 1	1	17	13	8.4	
	3	14	9.1	7.0	
	6	7.5	5.1	4.5	4
8 : 2	1	22	16	11	
	3	15	9.8	8.4	
	6	7.7	5.1	4.5	5
7 : 3	1	23	16	11	
	3	15	11	8.4	
	6	8.0	5.7	4.2	5

* Upon irradiation with 365-nm light (4.4 × 10^{-2} einstein dm^{-3} h^{-1}).

the acetylacetone procedure.[20] All procedures for calorimetric analysis were carried out after decolouration of the blue colour due to W^V by admission of oxygen, and blanks were prepared with solutions kept in the dark.

The evacuation to 10^{-4} Torr of solutions for both e.s.r. spectral measurement and flash photolysis was carried out by several freeze–pump–thaw cycles. *X*-Band e.s.r. spectra were recorded on a Varian E12 spectrometer. Solutions for electrochemical measurements were flushed with nitrogen to exclude oxygen. For controlled-potential reduction experiments, platinum net, wire, and silver wire were used as working, counter, and reference electrodes, respectively. All electric potentials are with reference to Ag–AgCl. Polarograms were recorded on EG & G PAR (174A and 303) instruments and a standard cell with a Ag–AgCl reference electrode. The photocurrent was measured potentiostatically using a bright platinum circular plate (area 18 mm^2) as a working electrode. The action spectrum of the photocurrent (plot of photocurrent per number of incident photons as a function of wavelength) was normalized to constant photon density, according to a previous method.[6] The flash-photolysis experiment was carried out using a Xenon Corp. model 720 flash-photolysis apparatus. Two EP-5-100C lamps were fired at 320 J per pulse. The lifetime for the flash pulse was 100 μs. A transmitting glass filter (Toshiba VY-43, cut-off $\lambda \leqslant 430$ nm) was inserted between the monitoring lamp and the reaction cell.

Results

Continuous Photolysis and E.S.R. Spectra.—Irradiation with 365-nm light of deaerated solutions containing $[NBu_4]_4[W_{10}O_{32}]$ in CH_3CN resulted in the prompt development of the blue colour due to photoabsorption in the intervalence charge-transfer (W^V–O–W^{VI} $\longleftrightarrow$ W^{VI}–O–W^V) bands of reduced decatungstates.[15,21] Figure 1 shows absorption changes in a typical irradiation experiment. The shape of the spectrum changes with the irradiation time, showing the formation of a blue species with $\lambda_{max.} = 780$ nm and subsequent formation of another blue species with $\lambda_{max.} = 630$ nm. Introduction of oxygen into the cuvette brought about the reoxidation of reduced decatungstates to $[W_{10}O_{32}]^{4-}$ and the absorption spectra of reoxidized solutions were identical with those prior to photolysis. The ion $[W_{10}O_{32}]^{4-}$ accepted more than one electron (nearly two) in long-term photolyses. Table 1 shows quantum yields (φ) of the photoproducts; φ for the formation of volatile and non-volatile products decreased with increasing duration of the irradiation, possibly due to an absorbance of the blue complex which is not photosensitive. The dominant oxidation product was 1-butene which is the one-electron oxidation product of $[NBu_4]^+$. Butyraldehyde product was also isolated in acetonitrile–water but not in the absence of water. Tungsten(V), 1-butene, and butyraldehyde as photoproducts in acetonitrile–water were formed approximately in a 10 : 7 : 0.5 molar ratio. A small amount of tributylamine was formed, less than 1% of that of 1-butene. The difference between the total number of equivalents of W^V and the number of equivalents of 1-butene formed implies the formation of other undetected oxidized species. Succinonitrile, the two-electron oxidation product of CH_3CN, was detected but we did not attempt to evaluate φ for the formation of solvent-derived products, since the values were believed to be very small ($\varphi < 10^{-5}$).

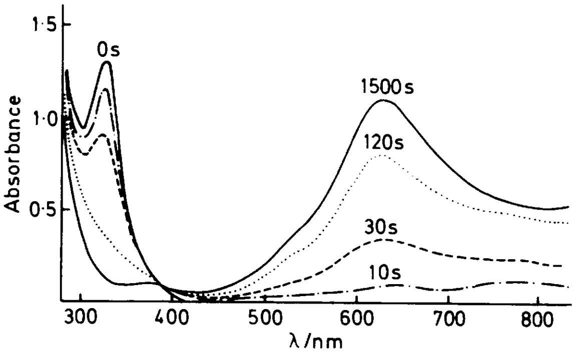

Figure 1. Absorption spectra of a deaerated solution containing 9.5 × 10^{-5} mol dm^{-3} $[NBu_4]_4[W_{10}O_{32}]$ in CH_3CN upon irradiation with 365-nm light at room temperature. Times (s) are indicated on the curves. Optical pathlength of the cell is 10 mm

The photolyte exhibited an e.s.r. signal at 77 K due to W^V, which consisted of a single isotropic line ($g = 1.84$, linewidth $\Delta H_{ms} = 20$ G) without hyperfine structure. This signal was not observed at room temperature. E.s.r. spectra for solutions containing 0.1 mmol dm^{-3} $[NBu_4]_4[W_{10}O_{32}]$ in CH_3CN were recorded at various stages of the photoreduction to one- and two-electron blues. The results are shown in Figure 2. The signal intensity increased continuously as the reduction proceeded up to *ca.* 1.5 electrons added to $[W_{10}O_{32}]^{4-}$ and then decreased with further reduction to 1.8 electrons. Assuming that the two-electron blue species is diamagnetic because of pairing of the second electron added to the polyoxo-anion with the first one due to superexchange interaction,[22] the decrease in e.s.r. signal intensity at the 1.8-electron stage of photoreduction can be explained by the eventual decrease in the concentration of the one-electron blue species due to the large extent of its conversion into the two-electron blue species.

Table 2. Quantum yields of photoproducts for deaerated solutions containing 3 mmol dm^{-3} $[NBu_4]_4[W_{10}O_{32}]$ and various concentrations of alcohols

Solvent composition acetonitrile–alcohol (v/v)		Irradiation time (h)	$10^2 \varphi_{W^V}$	$10^2 \varphi_{CHO}$	$10^5 \varphi_{1\text{-butene}}$
CH_3CN–BuOH	9 : 1	1	9.7	5.1	
		2	5.7	2.9	
		3	4.1	2.3	
		6	2.1	1.1	0
	9.5 : 0.5		1.0	0.4	2
	8 : 2		3.3	1.8	0
	7 : 3		5.0	2.5	
CH_3CN–MeOH	9 : 1		1.6	0.6	3
	7 : 3		2.2	1.1	0
	5 : 5		4.0	1.9	

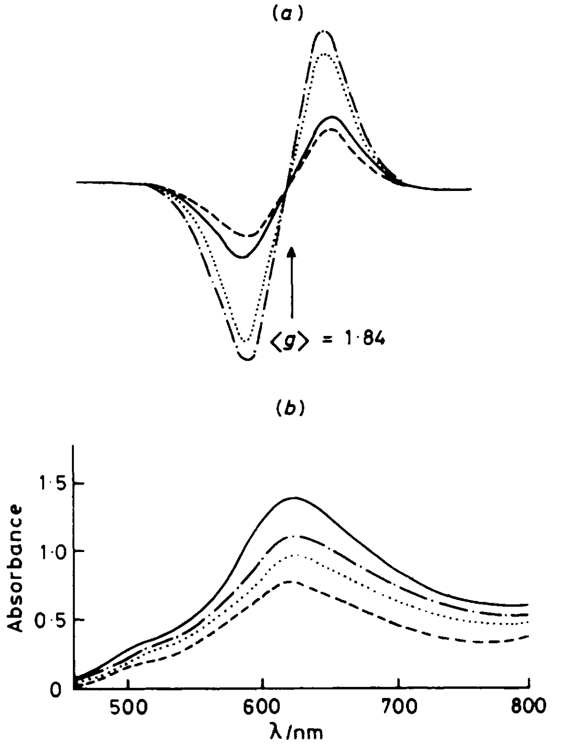

Figure 2. E.s.r. spectra at 77 K (*a*) and absorption spectra (*b*) of deaerated solutions containing 0.1 mmol dm^{-3} $[NBu_4]_4[W_{10}O_{32}]$ in CH_3CN at various stages of photoreduction: 0.5 (– – – –), 1.0 (· · · ·), 1.5 (— · —), and 1.8 (——) electrons added to $[W_{10}O_{32}]^{4-}$. Optical pathlength for absorption spectrum is 10 mm at room temperature

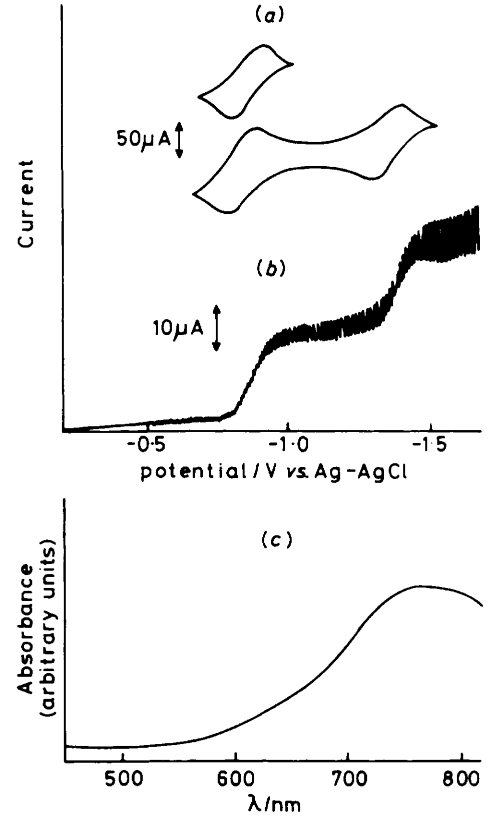

Figure 3. Electrochemical reduction of 1 mmol dm^{-3} $[NBu_4]_4[W_{10}O_{32}]$ in CH_3CN at room temperature: (*a*) cyclic voltammetry at a graphite electrode (scan rate 17 mV s^{-1}); (*b*) d.c. polarogram; (*c*) absorption spectrum of the blue species produced by controlled-potential reductions at −1.0, and −1.5 V *vs.* Ag-AgCl

U.v.-induced electron transfer from externally added alcohol to $[W_{10}O_{32}]^{4-}$ resulted in suppression of the photodegradation of $[NBu_4]^+$ (to 1-butene), and φ for tungsten(V) formation increased with increasing concentration of alcohol. In CH_3CN–BuOH ($\leqslant$ 9 : 1 v/v), the stoicheiometric amount of butyraldehyde was detected as shown in Table 2. A similar effect was observed when MeOH was added. In this case the stoicheiometric amount of formaldehyde was obtained in CH_3CN–MeOH ($\leqslant$ 7 : 3 v/v).

Electrochemistry.—Cyclic voltammetry of a solution containing 1 mmol dm^{-3} $[NBu_4]_4[W_{10}O_{32}]$ and 0.1 mol dm^{-3} $[NBu_4]ClO_4$ in CH_3CN revealed two successive nearly reversible diffusion-controlled reduction waves around −0.85 and −1.35 V *vs.* Ag–AgCl using a graphite electrode, as shown in Figure 3(*a*). The approximate reversibility of the reduction-oxidation steps was confirmed by a d.c. polarogram obtained with a dropping mercury electrode; this consisted of two well defined waves of signal height at the half-wave potential ($E_{\frac{1}{2}}$) of −0.94 and −1.37 V *vs.* Ag-AgCl, as shown in Figure 3(*b*). The plots of E *vs.* log $[(i_d - i)/i]$,* obtained from d.c. polarograms, were linear with slopes of 64 and 70 mV at 20 °C for the first and the second waves, respectively. Similar d.c. polarograms were observed in acetonitrile–water but $E_{\frac{1}{2}}$

---

* Where E, i, and i_d denote potential *vs.* Ag-AgCl, current, and diffusion-limited current.

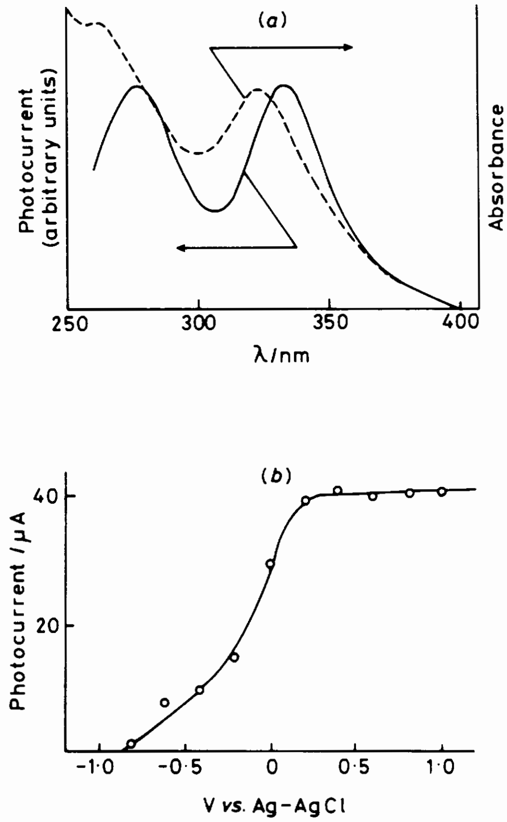

Figure 4. Anodic photocurrent at a platinum electrode for deaerated solution containing 1 mmol dm^{-3} $[NBu_4]_4[W_{10}O_{32}]$ and 0.1 mol dm^{-3} $[NBu_4]ClO_4$ in CH_3CN at room temperature: (*a*) action spectrum measured at 0.7 V *vs.* Ag–AgCl; (*b*) photocurrent–voltage curve upon irradiation with light at $320 < \lambda < 420$ nm. The absorption spectrum (— — —) of the sample solution is also shown in Figure 4(*a*) for comparison

Table 3. Half-wave potentials of $[W_{10}O_{32}]^{4-}$ in acetonitrile–water [a]

Solvent composition acetonitrile–water (v/v)	$E_{\frac{1}{2}}(1)$ [b]	$E_{\frac{1}{2}}(2)$ [b]
	V *vs.* Ag–AgCl	
10 : 0	−0.94	−1.37
9 : 1	−0.72	−0.96
8 : 2	−0.62	−0.81
7 : 3	−0.59	−0.74

[a] Solutions contain 5 mmol dm^{-3} $[NBu_4]_4[W_{10}O_{32}]$ and 0.1 mol dm^{-3} $[NBu_4]ClO_4$. [b] $E_{\frac{1}{2}}(1)$ and $E_{\frac{1}{2}}(2)$ are the cathodic half-wave potentials for the first and second waves, respectively.

Table 4. Onset potential (E_{onset}) of the anodic photocurrent in acetonitrile–water containing 5 mmol dm^{-3} $[NBu_4]_4[W_{10}O_{32}]$ and 0.1 mol dm^{-3} $[NBu_4]ClO_4$.

Solvent composition acetonitrile–water (v/v)	E_{onset}/ V *vs.* Ag–AgCl
10 : 0	−0.96
9.5 : 0.5	−0.84
9 : 1	−0.76
8 : 2	−0.63

shifted to more positive values as the concentration of water increased. The results are summarized in Table 3. Controlled-potential reductions of 1 mmol dm^{-3} $[NBu_4]_4[W_{10}O_{32}]$ at −1.0 and −1.5 V *vs.* Ag–AgCl in CH_3CN led respectively to the addition of one and two electrons per $[W_{10}O_{32}]^{4-}$. The absorption spectrum of the electrochemically reduced product exhibited a maximum at 780 nm and there was no significant difference in spectral shape in the visible region between $[W_{10}O_{32}]^{5-}$ and $[W_{10}O_{32}]^{6-}$, as shown in Figure 3(*c*). The e.s.r. spectrum of $[W_{10}O_{32}]^{5-}$ at 77 K was the same as for the photolyte in both *g* value and ΔH_{ms}. In the course of the controlled-potential reduction of $[NBu_4]_4[W_{10}O_{32}]$, no 1-butene could be detected.

Figure 4(*a*) shows the action spectrum of the steady-state photocurrent at 0.7 V *vs.* Ag–AgCl, which is due to the anodic ejection of the electron from the photoreduced species.[5,6] The spectral response shows the red shift of the charge-transfer band, compared with the absorption spectrum in CH_3CN. This suggests that the photocurrents originate from the photoabsorption of $[NBu_4]_4[W_{10}O_{32}]$ molecules adsorbed on the platinum electrode. Figure 4(*b*) shows the photocurrent–voltage curve in the same electrolyte. The onset of the photocurrent, which corresponds to the formal redox potential for the photoreduced species exhibiting the anodic photocurrent, begins around −0.8 V *vs.* Ag–AgCl. This value is similar to $E_{\frac{1}{2}}$ for $[W_{10}O_{32}]^{4-/5-}$ [Figure 3(*b*)]. Good correspondence between the onset potential of the anodic photocurrent and $E_{\frac{1}{2}}$ for $[W_{10}O_{32}]^{4-/5-}$ could also be observed in acetonitrile–water: the addition of water resulted in a shift of the onset potential to more positive values, as shown in Table 4. Furthermore, the photocurrent at the constant potential was linearly dependent on the light (340 nm) intensity, indicating that the formation of the photoreduced species exhibiting the anodic photocurrent comprises a one-photon process. These results suggest that the species exhibiting the anodic photocurrent is $[W_{10}O_{32}]^{5-}$.

Flash Photolysis.—Flash photolysis was carried out for deaerated solutions containing 0.1 mmol dm^{-3} $[NBu_4]_4[W_{10}O_{32}]$ in CH_3CN. The blue species with $\lambda_{max.} = 780$ nm appeared within the lifetime of the photoflash and decayed in part with a half-life of about 1 ms. At longer times a new absorption band appeared at 630 nm and increased in intensity over the course of about 30 s. Figure 5 shows (*a*) spectra obtained at 0.5 ms and 1 min, (*b*) the absorption change at 780 nm after the flash, and (*c*) the slow absorption increase at 630 nm. The transient spectrum observed at 0.5 ms after the flash is similar to the spectrum of the electrochemically reduced species, $[W_{10}O_{32}]^{5-}$ or $[W_{10}O_{32}]^{6-}$, in CH_3CN [Figure 3(*c*)]. In conjunction with the fact that the u.v.-induced e.s.r. signal due to the one-electron blue species developed in the course of the *ca.* 1.5-electron photoreduction of $[W_{10}O_{32}]^{4-}$ (Figure 2), the blue species with $\lambda_{max.} = 780$ nm observed during the flash pulse can be assigned as $[W_{10}O_{32}]^{5-}$. Continuous photolysis of $[NBu_4]_4[W_{10}O_{32}]$ in CH_3CN resulted in the formation of another blue species, with $\lambda_{max.} = 630$ nm, in addition to $[W_{10}O_{32}]^{5-}$ (Figure 1). Flash photolysis substantiates this observation.

Flash photolysis in the presence of water suppressed the slow development of the absorbance at 630 nm and no blue species with $\lambda_{max.} = 630$ nm was observed in acetonitrile–water (1 : 1 v/v). This allows a value of $\varepsilon_{780} = 1.1 \times 10^4$ dm^3 mol^{-1} cm^{-1} to be calculated for $[W_{10}O_{32}]^{5-}$. On the other hand, the addition of water produced no significant change in the transient absorption at 780 nm within 10 ms after the flash pulse.

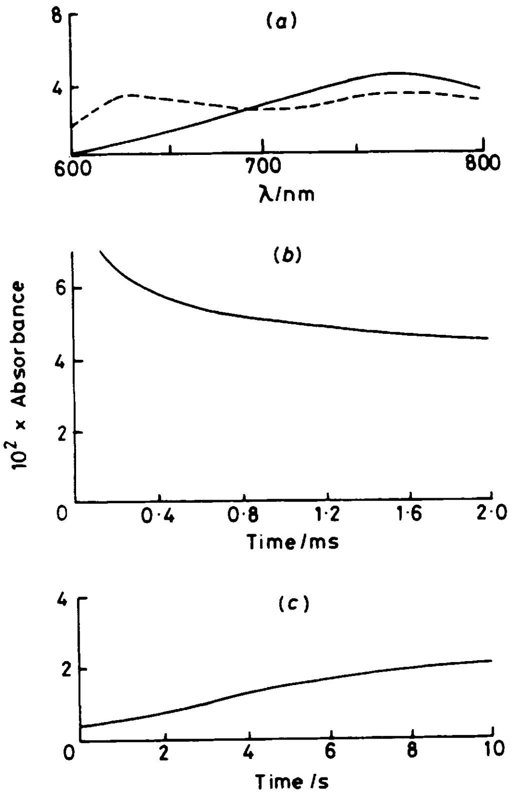

Figure 5. Blue species generated by flash photolyses of deaerated solutions containing 0.1 mmol dm^{-3} $[NBu_4]_4[W_{10}O_{32}]$ in CH_3CN at room temperature: (*a*) absorption spectra of the blue species obtained at 0.5 ms (——) and 1 min (- - - -) after the pulse; (*b*) transient absorbance at 780 nm; (*c*) transient absorbance at 630 nm. Optical pathlength of the cell is 11.7 cm

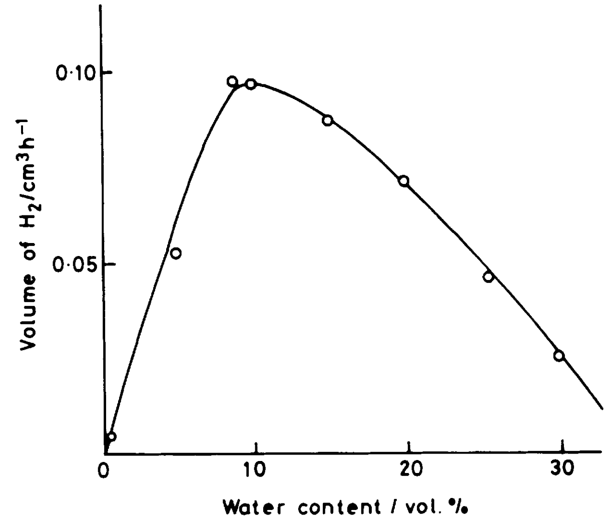

Figure 6. Variation in the amount of H_2 (cm^3 h^{-1}) photogenerated with water content at room temperature. The deaerated solutions (10 cm^3) contained 1.5 mmol dm^{-3} $[NBu_4]_4[W_{10}O_{32}]$ and 15 mmol dm^{-3} RuO_2 in acetonitrile–water. The amount of H_2 was measured after 1-h irradiation with light at $\lambda > 350$ nm

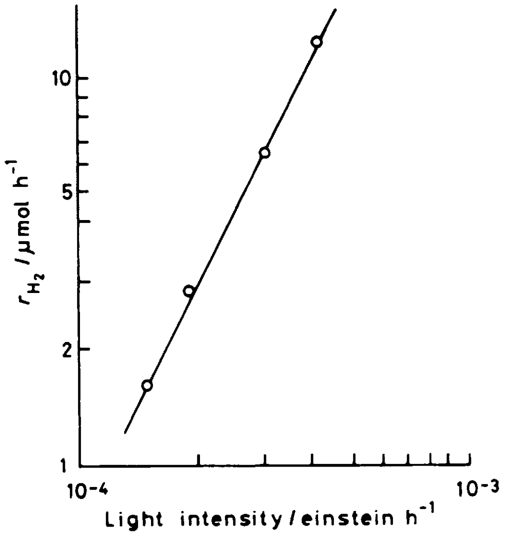

Figure 7. The rate of H_2 generation (r_{H_2}) as a function of 365-nm light intensity at room temperature. The deaerated solutions (10 cm^3) contained 1.5 mmol dm^{-3} $[NBu_4]_4[W_{10}O_{32}]$ and 15 mmol dm^{-3} RuO_2 in CH_3CN–BuOH (9 : 1 v/v)

Hydrogen Generation from Water and Alcohol.—From the fact that the formal potential of the $[W_{10}O_{32}]^{4-/5-}$ redox couple is sufficiently negative for the reduction of water (Tables 3 and 4), it is suggested that photocatalytic generation of H_2 from water and alcohol is possible by use of $[W_{10}O_{32}]^{4-}$. This could be indeed achieved with the help of heterogeneous catalysts such as Pt, RuO_2, and IrO_2. No H_2 generation was observed in the absence of heterogeneous catalysts. Figure 6 shows the amount of H_2 generated from solutions containing 1.5 mmol dm^{-3} $[NBu_4]_4[W_{10}O_{32}]$, 15 mmol dm^{-3} RuO_2, and various concentrations of water upon irradiation ($\lambda > 350$ nm) for 1 h, indicating that the optimum content of water in CH_3CN is 10%. Lowering of the amount of H_2 generated in higher contents of water may be ascribed to a positive shift of the formal potential of the $[W_{10}O_{32}]^{4-/5-}$ redox couple (Table 4). The H_2 evolution due to the water reduction was demonstrated by using D_2O: photolysis in CH_3CN–D_2O (9 : 1 v/v) yielded a gas comprising about 100% D_2, suggesting that D_2 originates from the reduction of D_2O rather than from hydrogen possibly adsorbed on the catalyst.

The effect of the light (365 nm) intensity on the rate of H_2 generation (r_{H_2}) was investigated for a solution containing 1.5 mmol dm^{-3} $[NBu_4]_4[W_{10}O_{32}]$ and 15 mmol dm^{-3} RuO_2 in CH_3CN–BuOH (9 : 1 v/v). The result is shown in Figure 7 where r_{H_2} is linearly dependent on the square of the light intensity, indicating that the step leading to H_2 generation is a two-photon process. The quantum yield for H_2 generation under these conditions was 0.03 after irradiation with 365-nm light (4.4 × 10^{-2} einstein dm^{-3} h^{-1}) for 3 h, and the catalytic turnover (defined as the ratio of the amount of hydrogen obtained to the initial amount of $[W_{10}O_{32}]^{4-}$) exceeded 100 at room temperature. Similar behaviour was observed in acetonitrile–water (9 : 1 v/v). In this case, however, the quantum yield (7 × 10^{-4}) for H_2 was extremely low, other experimental conditions being the same. Furthermore, the addition of heterogeneous catalysts to photolytes containing blue species in acetonitrile–water or -butanol brought about H_2 generation in the dark with concomitant reoxidation to $[W_{10}O_{32}]^{4-}$. The above results suggest that $[W_{10}O_{32}]^{4-}$ is important as a potential photocatalyst of H_2 production.

Discussion

U.v.-induced formation of $[W_{10}O_{32}]^{5-}$ and 1-butene (as a major photo-oxidation product) with $\varphi_{1\text{-butene}}/\varphi_{W^{v}} = 0.7$ in

CH_3CN reveals that a main step of the photolysis of $[NBu_4]_4[W_{10}O_{32}]$ is electron transfer from the positively charged $[NBu_4]^+$ to the negatively charged $[W_{10}O_{32}]^{4-}$ [equation (1)].

$$[NBu_4]^+ + [W_{10}O_{32}]^{4-} \xrightarrow{h\nu} [NBu_3^{\cdot}]^+ + [W_{10}O_{32}]^{5-} + H^+ + \text{1-butene} \quad (1)$$

The radical cation $[NBu_3^{\cdot}]^+$ may undergo deprotonation, disproportionation, and hydrolysis in the presence of water to yield butyraldehyde ($\varphi = 10^{-3}$—10^{-4}), tributylamine ($\varphi = 10^{-4}$—10^{-5}), and dibutylamine ($[NBu_3^{\cdot}]^+ \xrightarrow{-H^+} Bu_2N\dot{C}H\text{-}Pr \longrightarrow \frac{1}{2}NBu_3 + \frac{1}{2}Bu_2NCH{=}CHEt$, $Bu_2NCH{=}CHEt + H_2O \longrightarrow Bu_2NH + PrCHO$), although stoicheiometric amounts of the two amines were not verified experimentally.[23] The partial decay [Figure 5(*b*)] of the absorbance of $[W_{10}O_{32}]^{5-}$ at 780 nm obeyed a second-order process. Using $\varepsilon_{780} = 1.1 \times 10^4$ dm^3 mol^{-1} cm^{-1} for $[W_{10}O_{32}]^{5-}$ in combination with the slope of the second-order plot and with the optical path-length of the cell (11.7 cm), the rate constant for decay of $[W_{10}O_{32}]^{5-}$ was calculated to be 4×10^{10} dm^3 mol^{-1} s^{-1}. This value is near the diffusion-controlled limit and seems to be explicable in terms of the recombination of $[NBu_3^{\cdot}]^+$ and $[W_{10}O_{32}]^{5-}$ in the cage comprising the photoreaction site [equation (2)]. In reality, the recovery of the $[W_{10}O_{32}]^{4-}$

$$[NBu_3^{\cdot}]^+ + [W_{10}O_{32}]^{5-} \xrightarrow{k_2} NBu_3 + [W_{10}O_{32}]^{4-} \quad (2)$$

absorbance (not shown) was observed, but analysis of the absorbance kinetics was impossible because of a reduction in the signal-to-noise ratio obtained at u.v. wavelength corresponding to the photoabsorption of $[W_{10}O_{32}]^{4-}$. The detection of a small amount of NBu_3 ($\varphi = 10^{-4}$—10^{-5} in Table 1) is evidence in support of reaction (2), which effects a lowering of the quantum yield [$\varphi = (1$—$2) \times 10^{-2}$] of the W^V.

The blue species with $\lambda_{max.} = 630$ nm, which was produced in the course of continuous and flash photolyses [Figures 1 and 5(*c*)], was hardly observed on controlled-potential reduction in CH_3CN [Figure 3(*c*)]. A blue shift of the intervalence charge-transfer band has been reported for the protonation of the four-electron blue species of $[\beta\text{-}SiMo_{12}O_{40}]^{4-}$.[22] In conjunction with the conclusion that the reduction of $[W_{10}O_{32}]^{4-}$ to $[W_{10}O_{32}]^{5-}$, due to the photoredox reaction between $[W_{10}O_{32}]^{4-}$ and $[NBu_4]^+$ in CH_3CN, can be characterized by the deprotonation of $[NBu_4]^+$ [equation (1)], therefore, it is reasonable to assume that the blue species with $\lambda_{max.} = 630$ nm is protonated and that the slow absorption increase at 630 nm in the flash photolysis experiments [Figure 5(*c*)] can be attributed to the disproportionation of $[HW_{10}O_{32}]^{4-}$ {equation (3) where $[H_2W_{10}O_{32}]^{4-}$ denotes the two-electron reduced and diprotonated species}, since the intervalence band energies would be expected to be similar for $[HW_{10}O_{32}]^{4-}$ and $[H_2W_{10}O_{32}]^{4-}$.[22] Indeed, the slow increase in

$$2[HW_{10}O_{32}]^{4-} \xrightarrow{k_3} [H_2W_{10}O_{32}]^{4-} + [W_{10}O_{32}]^{4-} \quad (3)$$

absorption at 630 nm after the flash [Figure 5(*c*)] obeyed second-order kinetics. An average rate constant value, $k_3 = 6 \times 10^5$ dm^3 mol^{-1} s^{-1} in CH_3CN, was obtained using $\varepsilon_{630} = 1.8 \times 10^4$ dm^3 mol^{-1} cm^{-1} for $[H_2W_{10}O_{32}]^{4-}$, which was evaluated from the absorption spectrum of the photolyte corresponding to the addition of 1.8 electrons to $[W_{10}O_{32}]^{4-}$ (Figure 2).* Furthermore, a value $\varepsilon_{630} \approx 2 \times 10^3$ dm^3 mol^{-1} cm^{-1} was evaluated for $[HW_{10}O_{32}]^{4-}$. The possibility of disproportionation of $[W_{10}O_{32}]^{5-}$ is unlikely, because of the stronger electrostatic repulsion between the negative charges on non-protonated anions. The intensity of the e.s.r. signal in the continuous photolysis reached a maximum at *ca.* 1.5 electrons added to $[W_{10}O_{32}]^{4-}$ [Figure 2(*a*)]. The lack of a maximum at 1.0 electron is evidence in support of the regeneration of the photosensitive $[W_{10}O_{32}]^{4-}$ due to the disproportionation of $[HW_{10}O_{32}]^{4-}$ [equation (3)]; a further increase in the steady-state concentrations of $[W_{10}O_{32}]^{5-}$ and $[HW_{10}O_{32}]^{4-}$ would be required to attain the maximum in signal intensity due to the one-electron blue species. Accordingly, the development of the absorbance at 630 nm in the continuous and flash photolyses can be attributed to the formation of $[H_2W_{10}O_{32}]^{4-}$ due to the disproportionation of $[HW_{10}O_{32}]^{4-}$. The decrease in k_3 on addition of water to CH_3CN may be explained in terms of a corresponding decrease in the pK_a of $[HW_{10}O_{32}]^{4-}$, although we have not evaluated the latter parameter in CH_3CN. The addition of aqueous solutions (constant volume) of $HClO_4$ to CH_3CN enabled the pK_a of $[HW_{10}O_{32}]^{4-}$ to be estimated as *ca.* 3.7 in acetonitrile–water (9 : 1 v/v).

Controlled-potential reduction of $[W_{10}O_{32}]^{4-}$ has been reported [15] using $[NHBu_3]_4[W_{10}O_{32}]$ in propanediol 1,2-carbonate (pdc): one- and two-electron reductions of $[W_{10}O_{32}]^{4-}$ ($\varepsilon_{325} = 1.5 \times 10^3$ dm^3 mol^{-1} cm^{-1}) in pdc gave corresponding blue species and their absorption spectra ($\varepsilon_{max.} = 7.5 \times 10^3$ and 1.5×10^4 dm^3 mol^{-1} cm^{-1}) were similar to those of the blue species with $\lambda_{max.} = 780$ and 630 nm respectively, which were photochemically produced in CH_3CN. It may be recalled that the blue species with $\lambda_{max.} = 630$ nm was not observed under the controlled-potential two-electron reduction in CH_3CN [Figure 3(*c*)] and that $\varepsilon_{323} = 1.35 \times 10^4$ dm^3 mol^{-1} cm^{-1} for $[W_{10}O_{32}]^{4-}$, $\varepsilon_{780} = 1.1 \times 10^4$ dm^3 mol^{-1} cm^{-1} for $[W_{10}O_{32}]^{5-}$, and $\varepsilon_{630} = 1.8 \times 10^4$ dm^3 mol^{-1} cm^{-1} for $[H_2W_{10}O_{32}]^{4-}$ in CH_3CN differ from the values obtained in pdc. We cannot explain these discrepancies at present, although they may be due to the difference in solvent and distortions in the decatungstate structures.

In conjunction with the fact that the absorption kinetics at 780 and 630 nm for the flash photolysis in CH_3CN–BuOH were similar to those in acetonitrile–water, a reaction mechanism for the photocatalytic H_2 generation from BuOH is proposed based on the mechanism for the solution photochemistry of $[NBu_4]_4[W_{10}O_{32}]$ in CH_3CN [equations (4)—(8)]. The H_2 generation consisted of a two-photon process

$$[W_{10}O_{32}]^{4-} + BuOH \xrightarrow{h\nu} [W_{10}O_{32}]^{5-} + Pr\dot{C}HOH + H^+ \quad (4)$$

$$[W_{10}O_{32}]^{5-} + H^+ \longrightarrow [HW_{10}O_{32}]^{4-} \quad (5)$$

$$2[W_{10}O_{32}]^{5-} + 2H^+ \xrightarrow{\text{catalyst}} 2[W_{10}O_{32}]^{4-} + H_2 \quad (6)$$

$$[H_2W_{10}O_{32}]^{4-}\ [\textit{via}\ \text{equation (3)}] \xrightarrow{\text{catalyst}} [W_{10}O_{32}]^{4-} + H_2 \quad (7)$$

$$2Pr\dot{C}HOH \longrightarrow PrCHO + BuOH \quad (8)$$

(Figure 7). This excludes the possibility that one-electron oxidized (α-hydroxypropyl) radicals $Pr\dot{C}OH$ react with $[W_{10}O_{32}]^{4-}$, $[W_{10}O_{32}]^{5-}$, and $[HW_{10}O_{32}]^{4-}$ in the dark to produce the corresponding reduction products, since the rate of H_2 generation from BuOH would have been linearly dependent on the light intensity. Furthermore, H_2 generation by the reoxidation of both $[W_{10}O_{32}]^{5-}$ and $[H_2W_{10}O_{32}]^{4-}$ can be confirmed by the fact that addition of colloidal Pt or RuO_2 to the photolyte containing $[W_{10}O_{32}]^{5-}$ and $[H_2W_{10}O_{32}]^{4-}$ brought about a perfect recovery of $[W_{10}O_{32}]^{4-}$ with accom-

---

* Assuming that the absorbance at 780 nm in Figure 2 corresponds to the concentration of $[W_{10}O_{32}]^{5-}$, the net concentration of $[H_2W_{10}O_{32}]^{4-}$ is estimated by subtracting the amount of $[W_{10}O_{32}]^{5-}$ from the total amount of W^V.

panying formation of H_2 in the dark under deaerated conditions. Thus, the overall reaction mediated by $[W_{10}O_{32}]^{4-}$ can be expressed as in equation (9).[24] Similar H_2 generation

$$\text{BuOH} \longrightarrow \text{PrCHO} + \text{H}_2,\ \Delta G^{\ominus} = -8.8\ \text{kJ mol}^{-1} \quad (9)$$

was observed in the solvents CH_3CN–MeOH ($\leqslant 7:3$ v/v) and CH_3CN–EtOH ($\leqslant 7:3$ v/v). In these cases, equations (10) and (11) represent the overall endothermic reactions which as

$$\text{MeOH} \longrightarrow \text{HCHO} + \text{H}_2,\ \Delta G^{\ominus} = 2.1\ \text{kJ mol}^{-1} \quad (10)$$

$$\text{EtOH} \longrightarrow \text{CH}_3\text{CHO} + \text{H}_2,\ \Delta G^{\ominus} = 2.6\ \text{kJ mol}^{-1} \quad (11)$$

carried out involve simultaneous chemical conversion of photon energy.[24]

References

1 T. Yamase and T. Kurozumi, *J. Chem. Soc., Dalton Trans.*, 1983, 2205.
2 T. Yamase, *J. Chem. Soc., Dalton Trans.*, 1982, 1987; Y. Ohashi, K. Yanagi, Y. Sasada, and T. Yamase, *Bull. Chem. Soc. Jpn.*, 1982, **55**, 1254.
3 T. Yamase, R. Sasaki, and T. Ikawa, *J. Chem. Soc., Dalton Trans.*, 1981, 628; T. Yamase, *ibid.*, 1978, 283.
4 T. Yamase and T. Ikawa, *Bull. Chem. Soc. Jpn.*, 1977, **50**, 746; T. Yamase, H. Hayashi, and T. Ikawa, *Chem. Lett.*, 1974, 1055; T. Yamase, T. Ikawa, H. Kokado, and E. Inoue, *ibid.*, 1973, 615.
5 T. Yamase, *Inorg. Chim. Acta*, 1981, **54**, L165; 1982, **64**, L155; 1983, **76**, L25.
6 T. Yamase, *Inorg. Chim. Acta*, 1981, **54**, L207; T. Yamase and T. Ikawa, *ibid.*, 1979, **37**, L529; 1980, **45**, L55.
7 A. Moradpour, E. Amouyal, P. Keller, and H. Kagan, *Nouv. J. Chim.*, 1978, **2**, 547.
8 J. R. Darwent, P. Douglas, A. Harriman, G. Porter, and M. C. Richoux, *Coord. Chem. Rev.*, 1982, **44**, 83.
9 M. Grätzel, *Acc. Chem. Res.*, 1981, **14**, 376.
10 D. Duonghong, J. Ramsden, and M. Grätzel, *J. Am. Chem. Soc.*, 1982, **104**, 2977.
11 J. R. Darwent, *J. Chem. Soc., Chem. Commun.*, 1982, 798.
12 E. N. Savinov, S. S. Saidkhanov, V. N. Parmon, and K. I. Zamaraev, *React. Kinet. Catal. Lett.*, 1981, **17**, 407.
13 E. Papaconstantinou, *J. Chem. Soc., Chem. Commun.*, 1982, 12; E. Papaconstantinou, D. Dimotikali, and A. Politou, *Inorg. Chim. Acta*, 1980, **40**, 155.
14 E. Papaconstantinou and M. Z. Hoffman, *Inorg. Chem.*, 1982, **21**, 2087.
15 S. C. Termes and M. T. Pope, *Inorg. Chem.*, 1978, **17**, 500.
16 M. Boyer, *J. Electroanal. Chem., Interfacial Electrochem.*, 1971, **31**, 441.
17 M. Filowitz, R. K. C. Ho, W. G. Klemperer, and W. Shum, *Inorg. Chem.*, 1979, **18**, 93.
18 C. A. Parker, *Proc. R. Soc. London, Ser. A*, 1953, **220**, 104.
19 M. Pesez and J. Bartos, ' Colorimetric and Fluorimetric Analysis of Organic Compounds and Drugs,' Marcel Dekker, New York, 1974, p. 255.
20 Ref. 19, p. 152.
21 J. P. Launay and R. Massart, *J. Inorg. Nucl. Chem.*, 1976, **38**, 1627.
22 R. Massart, *Ann. Chim.*, 1969, **4**, 365.
23 P. J. Smith and C. K. Mann, *J. Org. Chem.*, 1969, **34**, 1821.
24 J. A. Dean (ed.), 'Lange's Handbook of Chemistry,' 11th edn., McGraw-Hill, New York, 1973, pp. 9–63.

Received 3rd June 1983; Paper 3/901